Published in final edited form as:
Dev Biol. 2007 January 15; 301(2): 404–416. doi:10.1016/j.ydbio.2006.09.005.

Xenopus Fibrillin Regulates Directed Convergence and Extension

Paul Skoglund[*,#] and **Ray Keller**[*]

[*]*Department of Biology, University of Virginia, Charlottesville, VA 22903 USA*

Abstract

Fibrillin- based human diseases such as Marfan Syndrome and Congenital Contractural Arachnodactyly implicate fibrillins in the function and homeostasis of multiple adult tissues. Fibrillins are also expressed in embryos, but no early developmental role has been described for these proteins. We use three independent methods to reveal a role for *Xenopus*fibrillin (XF) at gastrulation. First, expressing truncated forms of XF in the embryo leads to failure of gastrulation concomitant with a dominant negative effect on native fibrillin fibril assembly. Expressing truncated XF also inhibits normal progression of the patterned, polarized cell motility that drives convergence and extension at gastrulation, and perturbs directed extension in cultured explants of dorsal mesoderm. Second, injection of a synthetic peptide encoding a cell-binding domain of XF into mid-gastrula embryos causes acute failure of gastrulation associated with defective fibrillin fibril assembly. These injections also reveal a critical role for this peptide in the fibril assembly process. Third, morpholino-mediated knockdown of translation of XF in the embryo also perturbs normal gastrulation and directed extension. Together, these data show that native *Xenopus* fibrillin is essential for the process of directed convergent extension in presumptive notochord at gastrulation.

Keywords

Xenopus; Gastrulation; Fibrillin; Morphogenesis; Notochord

Introduction

Vertebrate gastrulation is a combination of two intertwined processes organized by Spemann's Organizer: morphogenetic tissue movements driven by patterned cell motility that remodel the embryo and the concomitant induction of specific cell fates, and these spatially and temporally regulated cellular behaviors are integrated over the entire presumptive notochordal/somitic region, or dorsal involuting marginal zone (DIMZ), to drive directed extension of this tissue along the anterior-posterior axis and ultimately the generation of a mature notochord flanked by segmented somites (Shih and Keller 1992a,b; Keller et al. 2000). The DIMZ is the "mechanical organizer" since these deformations drive gastrulation in the whole embryo, and cultured explants of DIMZ tissue (Keller explants) can autonomously undergo morphological extension to generate measurable force while anisotropically stiffening in the direction of extension (Moore et al., 1995). Regulation of cellular motility in the DIMZ is critical for this morphogenesis to occur, however, the locally acting molecular mechanisms that modulate

Corresponding Author: e-mail: ps5d@virginia.edu, phone: (434) 243-2596, Fax: (434) 982-5626, Address: University of Virginia, Department of Biology- Gilmer Hall Rm. 241, Charlottesville, VA 22903.

these behaviors to generate anisotropic tissue level forces remain poorly defined (Shih et al., 1992b; Keller et al., 2000).

Blastopore closure, most of involution at gastrulation, and elongation of the embryo during normal gastrulation are brought about by the posterior progression of expression of specific cell behaviors collectively called mediolateral intercalation behavior (MIB) (Keller, et al., 2000). DIMZ cells of the early gastrula are isodiametric and exhibit randomly directed protrusive activity but change their behavior during notochordal morphogenesis. These cells adopt both an elongated shape perpendicular to the axis of extension, and exhibit mediolaterally oriented bipolar protrusive activity (Shih and Keller, 1992a). Expression of MIB is induced in presumptive notochordal cells in an anterior-to-posterior and lateral-to-medial progression driving cell intercalation and leading to convergence (narrowing) and extension (lengthening) of notochord (convergent extension or CE) (Shih and Keller, 1992b). During this time, morphologically distinct structures composed of extracellular matrix (ECM) become apparent at the bilateral presumptive notochordal-somitic boundaries. These boundaries elongate from anterior-to-posterior concomitant with notochordal development, and are essential for the "boundary capture" mechanism of cell intercalation. An intercalating cell remains bipolar until it contacts the boundary, at which time it locally ceases the invasive intercalating type of protrusive activity at the boundary–contacting end. Instead, it spreads in the plane of the boundary and is stabilized or "captured" there, transiting to a monopolar protrusive mode while at the same time elongating the boundary (Shih and Keller, 1992b).

The first ECM component of the developing notochord-somite boundary is *Xenopus* fibrillin (XF) (Skoglund et al., 2006). Chick, mouse and human fibrillins are also found around notochords (Gallagher et al., 1993; Wunsch et al., 1994; Zhang et al., 1995; Rongish et al., 1998; Quondamatteo et al., 2002; Czirok et al., 2004). Human fibrillins –1, -2 and –3 (Fbns1-3) comprise a family of ECM glycoproteins that form filamentous microfibrils that both supply biomechanical support in the body and regulate signaling events. These proteins interact with cells through both integrin and proteoglycan receptors as well as ligands that include other ECM molecules and growth factors (reviewed in Robinson and Godfrey, 2000). Mutations in Fbn 1 and 2 are responsible for the human diseases Marfan syndrome (MFS) and congenital contractural arachnodactyly (CCA) and MFS patients have variable life expectancy that correlates with the severity of the allele inherited; some alleles exhibit a mild phenotype with near-normal lifespan while others are more severe, ranging to neonatal mortality (Dietz et al., 1994).

Here we examine the function of XF in the frog embryo by employing three distinct interdictions of fibrillin fibril assembly, all of which block normal progression of gastrulation in a manner consistent with a defect in axial morphogenesis. These data strongly implicate native XF fibrils at the notochord-somite boundary in the normal process of convergent extension of dorsal mesoderm during amphibian gastrulation, and additionally reveal a role for a conserved cell-binding domain in XF in fibril assembly.

Results

Expression of a truncation mutant of *Xenopus* fibrillin (XF) blocks gastrulation when expressed on the dorsal but not ventral sides of the gastrula

Targeted injection of synthetic mRNA encoding two amino-terminal truncated forms of XF, deletion-XF (delXF) and twice-deleted XF (TdXF), was performed into either the presumptive dorsal or ventral marginal zone of developing *Xenopus* embryos (Fig. 1A). These experiments were motivated by the observation that truncation alleles of human Fbn1 exert dominant negative effects on fibrillin deposition into matrix (See Schrijver et al., 2002). When expressed on the dorsal side of the gastrula, where native XF is expressed (Skoglund et al., 2006), normal

progression of gastrulation is blocked (Fig. 1B-G). In injected embryos the blastopore fails to close (Fig. 1C-G), leading to failure of normal internalization of mesoderm and lack of archenteron elongation. This failure is apparent first at late midgastulae stage (St.11), when dorsally injected embryos are retarded in closing their blastopores with respect to control injected animals (Fig. 1G, H). Failure of morphogenesis in injected animals is not due to a change in dorsal mesodermal cell fate, because notochord is still specified in injected animals (Fig. 1F). Notochordal tissue is found in a ring around the open blastopore, and appears similar to classic “ring embryos” generated by mechanically disrupting dorsal, axial tissue (Schechtman, 1942). In contrast, expression of deltaXF or TdXF on the ventral side of the blastopore leads to background levels of gastrulation defects, similar to expression of bovine pre-prolactin on the dorsal or ventral side (Fig. 1B).

Gastrulation blocking activity localizes to carboxy-terminal unique sequences

To address the molecular mechanism by which expressing amino-terminal deleted forms of XF on the dorsal side of the embryo perturbs gastrulation, we constructed two carboxy-terminal truncations of TdXF (Fig. 1A). One of these, TdXF-Protease (TdXF-P), is truncated at a putative furin protease processing site where fibrillins are normally cleaved by proteases during maturation (arrow in Fig. 1A). This truncation acts like the parent construct (TdXF) and blocks normal progression of gastrulation (Fig. 1B). In contrast, further deletion of carboxy-terminal unique sequences produces TdXF-Repeats (TdXF-R), which does not exhibit appreciable gastrulation blocking activity and thus implicates the unique sequences deleted from this protein in the molecular mechanism that perturbs gastrulation (Fig. 1B).

Explants of DIMZ expressing deltaXF extend abnormally

Since the phenotype of deltaXF/TdXF injected embryos and the localization of XF expression in the dorsal mesoderm are both consistent with involvement of XF in DIMZ convergent extension, we examined the effect of expressing deltaXF in DIMZ explants (Keller explants) which converge and extend autonomously. Keller sandwiches made from pairs of dorsal marginal zones of injected embryos do not extend properly. Notochords of approximately normal length and volume form in explants derived from injected animals, but these notochords are twisted and curled, and the severity of this phenotype depends on the dose of deltaXF RNA injected (Fig. 2A-D). These results suggest that deltaXF injections perturb the biomechanical mechanisms normally responsible for directed extension of this tissue.

To further explore this effect, we examined open face explants (derived from single embryos) unilaterally expressing deltaXF. These explants were assayed for bending, either towards or away from the injected side as determined by co-expression of green fluorescent protein (GFP). Sixty-nine percent (11 of 16) of deltaXF injected explants bent towards the injected side (Fig. 2E/F), and none bent away, suggesting that extension is retarded in deltaXF-expressing regions. In addition, a minority (25%) of these explants bifurcated between the notochord and somitic mesoderm at the site of expression (Fig. 2G/H arrowhead) suggesting a mechanical defect in deltaXF expressing tissue that could be due to altered matrix at the notochord-somite boundary. Only 6% of the experimental explants (1/16) extended in a straight manner. In contrast to the results with deltaXF, 73% of explants (11/15) unilaterally expressing control secreted proteins extended straight, neither bending or bifurcating, which is average for unmanipulated explants (unpublished observation REK).

deltaXF injected embryos exhibit a dominant interfering defect in wild type fibrillin localization to the boundary

To determine whether expression of deltaXF has a dominant effect on native XF localization or appearance, we examined native XF in open face explants mosaically expressing deltaXF. XF protein is normally concentrated at the notochord-somite boundary, and the JB3 antibody

used to visuallize XF does not detect the injection construct. This localization is clearly disrupted in regions co-expressing deltaXF and GFP, as reflected by a reduction of native fibrillin immunoreactivity at the boundary in expressing regions, while neighboring regions exhibit normal levels, localization and appearance of XF (Fig. 2E/F and G/H). In explants expressing deltaXF widely, native XF immunoreactivity is discontinuous and disorganized and often lacks orientation with respect to any embryonic axis, whereas in uninjected explants XF is continuous and aligned in two oriented stripes corresponding to the notochord-somitic boundaries (Fig. 2I, J).

Cells in the DIMZ expressing deltaXF behave abnormally during gastrulation

The dominant effect of deltaXF on convergence and extension could be due to an effect on the expression of MIB exhibited by the cells of the DIMZ responsible for convergent extension. To address this issue, we used low-light time lapse fluorescent video microscopy to follow individual, transplanted cells co-expressing deltaXF and GFP, or a control secreted protein (prolactin) and GFP, during extension of an open-faced explant in which the intercalating deep cells can be seen (Fig. 3A). In four such experiments, consistent behavioral differences were observed between these two cell populations. DeltaXF/GFP-expressing cells remained rounded and did not appreciably participate in MIB. When assayed at the conclusion of extension of the explant, only 3% of experimentally injected cells exhibit the elongated morphology normally adopted by cells that are expressing MIB (Fig. 3B-left side), compared to 53% of the pre-prolactin/GFP injected, transplanted cells in the same explants (Fig. 3B-right side). Consistent with a failure of MIB in deltaXF expressing cells, this population also showed reduced extension as shown by a reduction in the extension ratio (the anterior- posterior extent of the cell population at the conclusion of the experiment divided by the starting extent). Over three experiments, control injected cell populations exhibited an extension ratio of 1.69 ±0.27 (SEM), typical of open-faced explants at this stage (Shih and Keller, 1992a), whereas experimentally injected cell populations exhibited a ratio of 1.05 ±0.27. In addition, deltaXF expressing patches of cells do not intermingle with unlabeled host cells (Fig3B-left side), while control patches do intercalate with host tissue to generate mosaically labeled regions (Fig 3B-right side). DeltaXF expressing cells do not exhibit a generalized inhibition of motility, because both experimental and control injected head mesodermal cells exhibit characteristic migratory behaviors over the surface of the explant after transplantation (data not shown). Neither is this difference in behavior attributable to generalized cell sickness or to a nonspecific response in axial mesodermal cells to expression of deltaXF, because deltaXF-expressing cells obtained from regions adjacent to those transplanted adhere to and actively extend and retract lamellipodia when cultured on a fibronectin-coated plastic substrate (data not shown).

The cell binding region peptide (CB-1) inhibits gastrulation

Because the carboxy-terminal unique sequences of XF are required for the gastrulation arrest activity of TdXF (Fig. 1B), we evaluated the possible role of a putative heparin/cell binding protein motif (that we term cell binding 1 or CB-1) present in this region. CB-1 is similar in sequence to motifs in human fibrillins that are able to mediate cell attachment (Fig. 5B)(Ritty et. al. 2003), which overlap the multibasic site at which pro-fibrillins are matured by furin-class proteases. Injecting a synthetic peptide corresponding to the *Xenopus* CB-1 region into the blastocoel of developing gastrula stage embryos leads to a dramatic phenotype in which the normal progression of gastrulation is perturbed, similar to that seen in dorsally injected deltaXF embryos (Fig. 5A). CB-1 injected embryos fail to close their blastopores, to normally internalize axial mesoderm, and to elongate their archenteron. At stage 25, injected animals exhibit well-formed heads but almost completely lack trunks, leading to short, wide animals with open blastopores (Fig. 4A). This phenotype is not seen in parallel injections of a control peptide (Fig. 4B). Time-lapse video recordings of injected animals reveal a dramatic failure of mesodermal involution when they are injected during the second half of gastrulation when

axial morphogenesis is occuring (Fig. 4G). These movies reveal a gross change in the patterning of cell movements at gastrulation in injected embryos similar to that seen in embryos injected dorsally with deltaXF or TdXF, with mesoderm failing to internalize at the dorsal blastopore lip. When CB-1 peptide is injected at blastula stages, several hours before axial morphogenesis begins, no phenotype is observed until mid-gastrulation (data not shown).

CB-1 peptide blocks fibril assembly, which correlates with phenotype

To determine whether native XF fibrils are perturbed by CB-1 peptide injection, we stained injected animals for XF protein. Most injected embryos exhibit a severe phenotype, having a roughly spherical shape and a large open blastopore, with normal morphogenesis blocked from mid-gastrulation on. These embryos exhibit drastically reduced XF staining as compared to uninjected siblings (Fig. 4C). A few injected embryos that fail to close their blastopores exhibit some axial morphogenesis; they have elongated in the anterior-posterior direction and exhibit smaller open blastopores, and this correlates with increased XF staining along the developing axis (Fig. 4D). A minority of embryos are able to close their blastopores and exhibit both relatively normal development through gastrulation, and relatively normal XF staining, but often display pertubations in the normal pattern of XF deposition such as somitic staining on only one side of the embryo (Fig. 4E/F).

Characterizing the XF CB-1 functional domain

To define what sequences in the CB-1 peptide are required for gastrulation arrest activity, we produced an eight amino-acid carboxy-terminal deletion of this peptide (delCB-1). This peptide exhibits no gastrulation arrest activity when injected into the blastocoel of developing embryos (Fig. 5A). Five peptides representing point mutations in this region of the CB-1 peptide were made and assayed for gastrulation arrest activity, and none inhibited gastrulation when injected into the blastocoel of developing embryos (Fig. 5A/B). This region also overlaps the six amino acid predicted furin cleavage site that is the site of carboxy-terminal processing of pro-fibrillin into mature fibrillin. Importantly, each of these peptides represents an already cleaved product and therefore define this cluster of basic amino acid residues as bi-functional; required for the both for the gastrulation arrest activity exhibited by the CB-1 peptide and also important for directing proteolytic processing during maturation of intact fibrillins. Injecting a peptide that includes the 10 amino acids from XF past this protease site (CB1+10) leads to gastrulation arrest activity at similar frequency to CB-1 when injected on an equimolar basis, indicating that an intact protease site does not affect the gastrulation arrest activity of these peptides (Fig. 5A). A mutant version of this peptide, CB1+10M is analogous to the mutation in the CB-1M mutant peptide, and also fails to exhibit gastrulation arrest suggesting that the mechanism underlying gastrulation arrest activity is the same for both the CB-1 and the CB1 +10 peptides. In addition, because the mutation in the CB1 +10M peptide is expected to inhibit processing at the protease site we find no evidence for cell binding activity regulation by the state of proteolytic processing at this site.

Because the CB-1 region in Fbn 1 and 2 binds to cells in a heparin dependent manner (Ritty et al., 2003), we evaluated whether heparin can modulate the gastrulation arrest activity of the CB-1 peptide. Preincubating the CB-1 peptide with 200 μg/ml heparin before injection into the blastocoel markedly reduces the gastrulation arrest activity of CB-1, while similar injections of heparin without peptide do not affect gastrulation (Fig. 5D).

Cell behavior in presence of CB1 peptide

Expressing an amino-truncated form of XF containing the CB-1 region in DIMZ tissue at gastrulation perturbs the normal progression of cell behaviors thought to drive convergent extension in DIMZ tissue (Fig. 3B). To determine if the CB-1 cell-binding region is responsible for this effect on cell motility we challenged mature notochordal cells visualized in explants

undergoing morphogenesis with the CB-1 peptide. We find that the behavior of notochordal cells is not grossly affected by acute addition of the CB-1 peptide. When notochordal cells in axial explants at early neurula stages are challenged with the CB-1 peptide at 50 μg/ml their morphology does not change, exhibiting a length/width ratio of 2.5 at the beginning of the experiment and 2.4 at the end, consistent with normal notochordal cell behavior at neurula stages (Fig. 3C). The lack of a direct negative effect on the expression of notochordal cell behavior contrasts with the acute gastrulation arrest phenotype expressed by mid-gastrula embryos injected in the blastocoel with an equivalent dose of the same CB-1 peptide (Fig. 5A). We can not rule out that peptide access to the explant is less robust than peptide access in the embryo experiments and therefore leads to a lack of an observed peptide phenotype in explants, but view this as unlikely because the explants are made by removing both the ectodermal and endodermal epitheliums leaving just the deep neural layer opposed to the mesechymal mesodermal layer. These experiments suggest that the action of the CB-1 peptide that causes gastrulation arrest is distinct from the maintainance of notochordal cell behaviors.

Role of the CB-1 region in amino-terminal fragments of XF

Amino-terminal XF fragments exhibit two distinct activities in the developing embryo; a dominant negative effect on microfibril localization to the notochord-somite boundary, and an inhibitory effect on the progression of expression of cell motile behaviors in DIMZ tissue. Because injecting CB-1 peptide also interferes with microfibril organization, we wanted to understand the role of the CB-1 domain in the activity exhibited by amino-terminal XF fragments. To examine this issue we assayed the effect on developing embryos of a expressing a variant of TdXF-P lacking the eight amino acids shown to be required for CB-1 activity as a peptide (Fig. 5A), to reveal any second mode of action of these amino-terminal fragments that was independent of CB-1 region activity. We find that TXFdelCB1 does not exhibit gastrulation arrest activity above background when injected into the dorsal side of developing embryos (Fig. 5C).

Inhibiting XF translation leads to gastrulation arrest

Both ectopic expression of a dominant negative form of XF and injection of the CB-1 peptide block assembly of XF fibrils and disrupt gastrulation, and both treatments also are expected to increase the concentration of either monomeric XF or small, soluble aggregations of XF concomitant with fibril disruption. To determine the effect of reducing XF protein levels and thus inhibiting fibril formation without generating soluble fibrillin we used a morpholino complementary to XF coding sequences to inhibit translation of the XF protein in the developing frog. Injection of this XF morpholino, but not a control morpholino, both reduces the amount of XF protein made by the embryo (Fig. 6B), and perturbs the normal progression of gastrulation leading to a open blastopore phenotype similar to those seen with deltaXF/TdXF expression or CB-1 injection (Fig. 6A, C-E).

Because perturbing XF fibril assembly by expressing an amino-terminal deletion of XF on one side of a DMZ explant undergoing morphogenesis leads to bent or bifurcated explants, we assayed the effect of reducing XF translation on only one side of the embryo. At tailbud stage, eighty-eight percent of such injected embryos bend toward the injected side and none bent away (64/73 embryos), different than either the twelve percent of control morpholino injected embryos that bend (7/60 embryos; 5 towards and 2 away), or the seven percent of uninjected embryos that exhibit a bend of thirty degrees (5/74 embryos bent in either direction) (Fig. 6F/G).

Discussion

Xenopus Fibrillin (XF) is an ECM molecule that functions in convergent extension of dorsal, axial and paraxial mesoderm

We use three distinct methods to reveal a role for XF at gastrulation. We show that expression of amino-terminal deletions of XF in developing *Xenopus* embryo (deltaXF/TdXF), as well as injection of a peptide (CB-1) corresponding to a putative cell binding domain in XF into embryos, blocks normal progression of gastrulation and perturbs assembly of XF fibrils in the embryo. In addition, morpholino-mediated reduction of XF protein in the embryo causes a similar gastrulation phenotype. Because all three methods of perturbing XF lead to a similar embryonic phenotype in which morphogenesis at gastrulation is compromised, native XF protein function is required at gastrulation for normal development to occur.

Several observations argue that native XF functions in convergent extension of the dorsal mesoderm. Both XF RNA and protein are expressed at the right time, the midgastrula stage, and the right place, in the dorsal mesoderm that undergoes convergent extension or dorsal involuting marginal zone (DIMZ) (Skoglund et al., 2006). Expression of amino-terminal XF truncations blocks normal progression of gastrulation, and these effects are both temporally specific, occuring at the onset of native XF expression, and spatially specific, occuring when deltaXF/TdXF is expressed in dorsal but not ventral mesoderm. Similarly, injection of the CB-1 peptide into the blastocoel of developing embryos during convergent extension blocks normal gastrulation, with the level of matrix disruption correlating with severity of gastrulation phenotype. The CB-1 injection phenotype is also temporally specific, perturbing normal gastrulation within 30 minutes of injection into the blastocoel of embryos actively internalizing mesoderm, but when CB-1 is injected at earlier developmental stages no phenotype is seen until the onset of mesodermal involution at mid-gastrulation, concomitant with native XF expression.

The most direct evidence that XF is involved in mesodermal convergent extension is that Keller sandwiches expressing deltaXF exhibit dose-dependent curling, that open face explants unilaterally expressing deltaXF bend towards the injected side, and that reducing XF translation on one side of intact embryos also causes bending toward the injected side. In explants, extension is less vigorous in regions expressing deltaXF, compromising directed extension and providing a mechanical mechanism to explain failure of gastrulation in whole embryos, since axially directed convergent extension of the DIMZ drives normal blastopore closure and embryo elongation (Keller et al., 2000). Direct, high resolution analysis of cell motility of both control and deltaXF-expressing cells in these explants, co-labeled with GFP, show that the cell behaviors that drive convergent extension are inhibited by deltaXF, providing a cellular mechanism for the failure of convergent extension and the resulting arrest of gastrulation.

In whole embryos, the gastrulation phenotypes due to deltaXF/TdXF expression, CB-1 injection or morpholino injection are consistent with failure of convergent extension, rather than other processes in gastrulation. Convergent extension of the dorsal mesoderm is required for normal, asymmetric blastopore closure, DIMZ involution, and archenteron formation in intact embryos. It is these processes that fail in experimental embryos. Anterior to posterior progression of convergent extension of the notochordal and somitic mesoderm generates arcs of tension that bring about asymmetric involution and extension of the DIMZ, such that an elongated archenteron roof with overlying central notochord and bilateral somitic mesoderm is formed (Shih and Keller, 1992b). Local bilateral disruption of the arcs of convergent tissue in the DIMZ result in failure of involution and the open blastopore phenotype (Schechtman, 1942), similar to those produced here with deltaXF/TdXF, CB-1 or morpholino injection. A similar gastrulation arrest phenotype can be generated by expressing a dominant negative cadherin in the DIMZ (Lee and Gumbiner, 1995) and the zebrafish E-cadherin mutant

halfbaked exhibits a partially penetrant phenotype of bifucated notochords (Kane et al., 1996) suggesting that, as one might expect, multiple cellular and molecular functions are involved in the cellular rearrangements that mediate morphogenesis.

The alternative hypothesis, that deltaXF/TdXF expression, CB-1 peptide or mopholino injection affect processes other than convergent extension, such as bottle cell formation, migration of head mesoderm on the blastocoel roof, convergent extension of the neural tissue, or epiboly of the blastocoel roof itself, is not supported by our evidence. In the absence of any of these processes, singly or in combination, gastrulation proceeds without producing the phenotype we observe in these embryos; instead blocking these processes result in normal asymmetric blastopore closure and involution, and axial elongation (Keller and Jansa, 1992; Hardin and Keller, 1988; Keller et al., 2000).

Mechanisms underlying gastrulation arrest

Because both deltaXF/TdXF expression and CB-1 injection inhibit XF fibril formation and perturb gastrulation, similar to reducing XF protein levels in the embryo, the normal localization of near–normal levels of XF to the notochord –somite boundary is implicated as essential for successful gastrulation. Since this boundary plays a key role in convergent extension, disrupting XF protein localization in this region could affect convergent extension in several ways (Fig. 7A). First, the boundary has a short range, contact-mediated effect of inducing the monopolar cell behavior and the resulting "boundary capture" of the bipolar, mediolaterally intercalating cells (Shih and Keller, 1992b), Second, the bipolar MIB that drives convergent extension (Shih and Keller, 1992b), appears to be induced by signals emanating from the notochord-somite boundary (Domingo and Keller, 1995). A defective boundary could affect the cell motility underlying convergent extension, directly and locally in the first case, and indirectly in the second case. Third, the XF-containing boundary matrix could have a direct mechanical effect on convergent extension by contributing to the observed stiffening of the DIMZ along the anterior-posterior axis shown by compression, stress relaxation tests (Moore et al., 1995). Finally, this matrix may need to be intact to act as a mechanical integrator for morphogenesis of the DIMZ, incorporating all cells medial to the boundary into a single, unfractured and unbent, mature notochord.

Our results are consistent with a defect in one or more of these boundary functions, due to failure of fibrillin fibril assembly at the notochord-somite boundary. Because directed extension is perturbed in deltaXF injected explants, a mechanical role for XF fibrils at the notochord –somite boundary is strongly suggested by our data. Failure of directed extension would also fully explain the gastrulation arrest phenotypes generated with deltaXF/TdXF, CB-1 peptide or morpholino injection. In this model, XF fibrils serve as a substrate for MIB expressing cells, mechanically integrating the force generated by cell motility in the notochord into directed, posterior, extension while stiffening the axis. This model predicts that disrupting or reducing XF fibrils in the embryo will alter the biomechanical properties of the developing axis.

Our results also show that MIB is dramatically reduced specifically in deltaXF expressing regions, suggesting that mis-regulated XF fibril formation is capable of directly or indirectly regulating cell motility in the axis. Perturbing the patterned expression of cell motility could also cause gastrulation arrest in whole embryos. However, because we do not see a direct inhibitory effect on MIB due to the CB-1 peptide, a failure of a mechanical role for XF fibrils is likely the primary defect in CB-1 injected embryos, whereas in deltaXF/TdXF injected embryos we have evidence that disruption of both a mechanical role for fibrils in the boundary as well as mis-regulation of local cell motility combine to produce the gastrulation arrest phenotype. In combination, these data suggest that the native XF fibrils serve at least two

functions at gastrulation, acting both to mechanically integrate local cell motility in order to translate it into tissue level directed extension, as well as to regulate this local cell motility.

Role for the CB-1 domain

Both deltaXF/TdXF expression and CB-1 peptide injection affect convergent extension; because deletion of the CB-1 domain from TdXF removes this activity this domain appears to be central to the gastrulation phenotype in both cases. The observation that the 17-mer CB-1 homology domain from human Fbn 1 supports cell attachment to a wide variety of cells indicates the presence of a widely expressed but as yet unidentified receptor (Ritty et al., 2003). Because this cell attachment can be competed with heparin, and can be blocked by pretreating cells with heparitinase II, this receptor is likely a cell surface heparan sulfate proteoglycan. In cell culture, Fbn 1 and 2 fibril assembly can be blocked with soluble heparin, and these molecules each have several distinct heparin binding sites, including the CB-1 homology domain (Tiedemann et al., 2001; Ritty et al., 2003). Assembly requires specific cell types, suggesting a role for an unidentified receptor (Dzamba et al., 2001), and generates fibrillin molecules arrayed in a head-to tail fashion in microfibrils suggesting the presence of at least two multimerization domains per molecule (Reinhardt et al., 1996). We propose that the CB-1 domain on XF mediates heparin-dependent binding to a site on cell surfaces, that this is an obligate step in the process of fibril assembly, and that the mechanism of action of the CB-1 peptide is to block this interaction and thus fibril assembly. This view is strongly supported by our observation that pretreating CB-1 peptide with heparin reduces its gastrulation arrest activity.

A human MFS Fbn 1 allele with a point mutation in the CB-1 homology domain (R2726W, analogous to the mutant CB-1 peptide CB1-R6W in this study) supports the notion that the CB-1 domain is critical for Fbn assembly (Milewicz et al., 1995). This family presents an extremely mild form of MFS, and may represent the null phenotype. Dermal fibroblasts cultured from one of these patients produce and secrete normal amounts of Fib-1 protein, but exhibit half of normal Fib-1 deposition into matrix, implicating a functional CB-1 homology domain in fibril assembly. Because this mutation is in the consensus furin processing site at the Fbn 1 carboxy-terminal and inhibits proteolytic processing, this has been interpreted as evidence that carboxy-terminal processing is required for assembly into the matrix. However, this does not explain why this allele does not exhibit a dominant negative activity leading to more severe MFS, since premature termination Fbn 1 alleles exhibit dominant negative effects on fibrillin assembly into matrix (Schrijver et al., 2002). We suggest that in addition to a processing defect this R2726W mutant also fails to interact with a cell surface receptor through its CB-1 domain, and this is the reason this allele both does not assemble into matrix and does not exhibit dominant negative activity.

Molecular mechanism of action for amino-terminal XF deletions

Amino-terminal XF truncations that contain the CB-1 domain also perturb gastrulation, and this domain may be functioning to block fibril assembly in a manner analogous to what we envision for CB-1 peptide injection. This view is strongly supported by the observation that expressing TdXF-del8 in embryos, in which the CB-1 domain is inactivated, does not cause gastrulation arrest. However, deltaXF/TdXF expression also perturbs the normal progression of cell behaviors in the dorsal axis, and this phenotype is not recapitulated by soluble CB-1 peptide. We suggest that this phenotype is due to the production of “mini-fibrils”, consisting of native, full-length fibrillin associated with the amino-terminal truncated deltaXF/TdXF protein product, which are not created when the CB-1 peptide in injected. We hypothisize that these minifibrils are responsible for the inhibition of expression of MIB in injected regions that we observe in deltaXF injected regions. Because fibrillins exhibit integrin binding activity (Robinson and Godfrey, 2000) through domains that are absent in the deltaXF/TdXF

constructs, integrin binding activity of native fibrillin molecules assembled into minifibrils may mediate this effect. One normal function of the notochord-somite boundary is to induce local inhibition of protrusive activity (Shih et al. 1992b); we suggest that fibrillin normally mediates this inhibition at the boundary and that minifibrils also exhibit this activity but are mislocalized away from the boundary, leading to the observed inhibition of MIB cell motility in deltaXF/TdXF expressing regions.

Multiple roles for fibrillin at gastrulation

At gastrulation, XF is expressed specifically in DIMZ tissue undergoing morphogenesis, and is localized to the presumptive notochordal-somitic boundaries as microfibrils. The transformation of the short but wide presumptive notochordal region into a one cell wide, elongated notochord occurs by progressive anterior to posterior and lateral to medial expression of both mono-and bi-polar cell intercalation behavior, which results in pulling the boundaries medially, "zipping up" of the notochord field, and extension in the posterior direction (Fig. 7A). Here we present evidence that XF fibrils in the notochord-somite boundary serve as mechanical integrators of this cell behavior in dorsal, axial tissue, required for directed extension of dorsal mesoderm. In this model, the XF matrix imparts a mechanical stability to the extending boundary, and deltaXF/TdXF expression, CB-1 application or reduction of XF levels may generate a mechanically weak matrix, prone to fracture when subjected to use as a substrate for cell spreading or as a mechanical integrator during notochord formation. This results in the bent and multiple notochord phenotypes (Fig 7B,C). A second role for XF consistent with this work is as a signal to notochordal cells that they are at the notochord-somite boundary, leading these cells to locally cease protusive activity and transit from bipolar to monopolar protrusiveness. We postulate that interaction with truncated XF spatially misregulates this activity of native XF, this hypothesis remains to be tested. Microfibrils are also capable of modulating signal transduction (Arteaga-Solis et al., 2001; Charbonneau et al., 2004); but because dorsal cell fates are not perturbed in these experiments no such role was uncovered here. In combination, three distinct interdictions reveal XF fibrils are required for gastrulation, and suggest that this requirement operates at several levels including (1) as an ECM substrate for notochordal cells responsible for mechanically integrating local cell motility into tissue-level directed force, (2) as a stiffening element in the developing axis, and (3) as a signaling center, regulating cell motility in and around the notochordal-somite boundary.

Materials and Methods

Embryos, manipulations, immunochemistry and Western

Both pigmented and albino *Xenopus* embryos were generated by conventional techniques, and sandwich and open-face DIMZ explants were made from stage 10 embryos and cultured as described (Skoglund et al., 2006). Dorsal, axial explants were made from St. 14 embryos by removing the superficial endodermal epithelium to reveal the notochord. Transplantation studies involved making DIMZ explants from injected animals and transplanting a small number of both control and experimentally injected notochordal cells into a naive host and re-explanting into culture, and this host explant converges and extends (see Fig 3A.) Both groups of transplanted cells express GFP so these cells can be followed in the context of the morphogenesis of the host explant, and MIB is assayed by cell morphology while mediolateral intercalation of transplanted cells is inferred by the relative breakup of the transplanted group of cells in the context of the morphogenesis of the host explant (Fig 3B- Control cells on right side of arrowheads, experimental cells on left side). Other expressing cells from these explants were plated on dots created by allowing 10 μls of 100 μg/ml fibronectin to dry on a culture dish. Fibrillin and notochord were detected with the monoclonal antibodies JB3 (Rongish et al., 1998) and Tor7, respectively, by standard techniques (Skoglund et al., 2006). Western

blotting was performed and quantitated as described using the JB3 antibody to detect XF, and a cross-reacting band running at 200 kD is used as a loading control (Skoglund et al., 2006).

Production of constructs, and RNA Preparations and Microinjections

Capped mRNA was prepared utilizing the Maxiscript kit (Ambion). DeltaXF (linearized with EcoRI and transcribed with SP6) was constructed by subcloning a 4.4 kb BamHI-EcoRI fragment from pXND4 (Skoglund et al., 2006) into BamHI-EcoRI cut N-CadΔE (Kintner et al., 1992), resulting in an in frame fusion of 30 amino acids of N-cadherin signal sequence ahead of carboxy-terminal XF coding sequences. TdelXF (EcoRI/SP6) was constructed by replacing a BamHI-ApaI fragment with a PCR product generated with ATAGGATCCGGGGAGCAAAAGCTTATTTCTGAGGAGGATCTG CATCATCATCATCATCAT / gacacagatgtagc), removing 17 amino acids encoding a partial EGF repeat including potentially unpaired cysteine residues present in deltaXF. Carboxy terminal deletions of TdelXF were constructed by removing a BstII- NsiI fragment and replacing it with PCR products generated with (TCTTGCATTGATAACAATG / catatatgcatcatcctgagacacagtgcccttg) to generate TdelXF-R and (TCTTGCATTGA TAACAATG / atgatatcatcatcctcgcttggggtacccatt) for TdelXF-P, while TXF-delCB1 was constructed by replacing a KpnI-EcoRI fragment with a PCR product generated with (TCAATGGGTACTAGCCCAAGAAAGGAAGGCAGAGGCGAAATGCAGATGAC / gtaatacgactcactataggg). RNA encoding bovine pre-prolactin was from pSP35T (SP6/EcoRI), Green Fluorescent Protein was from pRN3GFP (T3/SFI1), or the S65T mutant pcs2t/S65T (SP6/Not1), and the membrane localized form of GFP was from GAP-43-GFP (SP6/NotI). Embryos were injected with 5- 20 nl of 50-200 ng/μl RNA in water in 1 or 2 blastomeres at the 2 or 4-cell stage, and dorsal or ventral marginal zone targeting was accomplished by using pigment cues (Lee and Gumbiner, 1995).

Immunochemistry, Peptides and Morpholinos

Custom synthetic peptides (Synpep or Invitrogen) were resuspended at 10 mg/ml in water. Injection was of 300 ng peptide/embryo into the blastocoel of developing embryos at stage 11 for all 17-mer peptides, and 450 ng peptide/embryo for all 27-mer peptides to maintain similar molarities. A morpholino complementary to XF was produced (gcctatgttatatgaacagcagca) (Genetools, Inc.) as well as a control morpholino (gcgtatcttatatcaagagcagga) that varies at five nucleotides. Injection was of 5 nl of 1 mM morpholino in one or both blastomeres at 2 cell stage to achieve 10 uM morpholino in the embryo. Injection protocol was as above, and embryos were cultured in 2/3 MBS at room temperature. Unilateral injections included 50 ng ruby- labelled dextran (Molecular Probes D-1817) as a tracer. Embryos were dissected out of their vitelline membranes, cultured at least two hours to allow them to straighten and then scored as bent if they exhibit a persistent axial bend of at least 30 degrees using fluorescence to determine if bend is toward or away from the injected side.

Time lapse video

Low light fluorescence video microscopy was done with either a Nikon Diaphot or a Nikon IX70 inverted microscope, using high numerical aperture 10, 20 and 60x fluorescence objectives. Imaging was done with a Hammatsu SIT camera, model 2400-08, or model C4742-95. Image processing was accomplished using Image1 or Metamorph software (both Universal Imaging) and images were post-processed using ImageJ (NIH) or Photoshop (Adobe). Confocal imaging was performed with a Nikon IX70 with a BioRad laser head and software at the Keck Center for Cellular Imaging at UVA. Framing intervals of 30 sec to 3 min were used and image processing consisted of frame averaging and brightness and contrast adjustment as described previously (Shih and Keller, 1992a).

References

Arteaga-Solis E, Gayraud B, Lee SY, Shum L, Sakai L, Ramirez F. Regulation of limb patterning by extracellular microfibrils. J Cell Biol 2001;154:275–81. [PubMed: 11470817]

Charbonneau NL, Dzamba BJ, Ono RN, Keene DR, Corson GM, Reinhardt DP, Sakai LY. Fibrillins can co-assemble in fibrils, but fibrillin fibril composition displays cell-specific differences. J Biol Chem 2003;278:2740–9. [PubMed: 12429739]

Corson GM, Charbonneau NL, Keene DR, Sakai LY. Differential expression of fibrillin-3 adds to microfibril variety in human and avian, but not rodent, connective tissues. Genomics 2004;83:461–72. [PubMed: 14962672]

Czirok A, Rongish BJ, Little CD. Extracellular matrix dynamics during vertebrate axis formation. Dev Biol 2004;268:111–22. [PubMed: 15031109]

Dietz HC, Mecham RP. Mouse models of genetic diseases resulting from mutations in elastic fiber proteins. Matrix Biol 2000;19:481–8. [PubMed: 11068202]

Dietz HC, Ramirez F, Sakai LY. Marfan's syndrome and other microfibrillar diseases. Adv Hum Genet 1994;22:153–86. [PubMed: 7762452]

Domingo C, Keller R. Induction of notochord cell intercalation behavior and differentiation by progressive signals in the gastrula of Xenopus laevis. Development 1995;121:3311–21. [PubMed: 7588065]

Dzamba BJ, Keene DR, Isogai Z, Charbonneau NL, Karaman-Jurukovska N, Simon M, Sakai LY. Assembly of epithelial cell fibrillins. J Invest Dermatol 2001;117:1612–20. [PubMed: 11886530]

Gallagher BC, Sakai LY, Little CD. Fibrillin delineates the primary axis of the early avian embryo. Dev Dyn 1993;196:70–8. [PubMed: 8334300]

Hardin J, Keller R. The behaviour and function of bottle cells during gastrulation of Xenopus laevis. Development 1988;103:211–30. [PubMed: 3197630]

Kane DA, Hammerschmidt M, Mullins MC, Maischein HM, Brand M, van Eeden FJ, Furutani-Seiki M, Granato M, Haffter P, Heisenberg CP, Jiang YJ, Kelsh RN, Odenthal J, Warga RM, Nusslein-Volhard C. The zebrafish epiboly mutants. Development 1996;123:47–55. [PubMed: 9007228]

Keller R, Davidson L, Edlund A, Elul T, Ezin M, Shook D, Skoglund P. Mechanisms of convergence and extension by cell intercalation. Philos Trans R Soc Lond B Biol Sci 2000;355:897–922. [PubMed: 11128984]

Kielty CM, Baldock C, Lee D, Rock MJ, Ashworth JL, Shuttleworth CA. Fibrillin: from microfibril assembly to biomechanical function. Philos Trans R Soc Lond B Biol Sci 2002;357:207–17. [PubMed: 11911778]

Kintner C. Cadherins and the morphogenesis of epithelial tissues in Xenopus embryos. Cold Spring Harb Symp Quant Biol 1992;57:335–44. [PubMed: 1285054]

Lee CH, Gumbiner BM. Disruption of gastrulation movements in Xenopus by a dominant-negative mutant for C-cadherin. Dev Biol 1995;171:363–73. [PubMed: 7556920]

Milewicz DM, Grossfield J, Cao SN, Kielty C, Covitz W, Jewett T. A mutation in FBN1 disrupts profibrillin processing and results in isolated skeletal features of the Marfan syndrome. J Clin Invest 1995;95:2373–8. [PubMed: 7738200]

Moore SW, Keller RE, Koehl MA. The dorsal involuting marginal zone stiffens anisotropically during its convergent extension in the gastrula of Xenopus laevis. Development 1995;121:3131–40. [PubMed: 7588048]

Quondamatteo F, Reinhardt DP, Charbonneau NL, Pophal G, Sakai LY, Herken R. Fibrillin-1 and fibrillin-2 in human embryonic and early fetal development. Matrix Biol 2002;21:637–46. [PubMed: 12524050]

Raghunath M, Putnam EA, Ritty T, Hamstra D, Park ES, Tschodrich-Rotter M, Peters R, Rehemtulla A, Milewicz DM. Carboxy-terminal conversion of profibrillin to fibrillin at a basic site by PACE/furin-like activity required for incorporation in the matrix. J Cell Sci 1999;112 (Pt 7):1093–100. [PubMed: 10198291]

Reinhardt DP, Gambee JE, Ono RN, Bachinger HP, Sakai LY. Initial steps in assembly of microfibrils. Formation of disulfide-cross-linked multimers containing fibrillin-1. J Biol Chem 2000;275:2205–10. [PubMed: 10636927]

Ritty TM, Broekelmann TJ, Werneck CC, Mecham RP. Fibrillin-1 and -2 contain heparin-binding sites important for matrix deposition and that support cell attachment. Biochem J 2003;375:425–32. [PubMed: 12837131]

Robinson PN, Godfrey M. The molecular genetics of Marfan syndrome and related microfibrillopathies. J Med Genet 2000;37:9–25. [PubMed: 10633129]

Rongish BJ, Drake CJ, Argraves WS, Little CD. Identification of the developmental marker, JB3-antigen, as fibrillin-2 and its de novo organization into embryonic microfibrous arrays. Dev Dyn 1998;212:461–71. [PubMed: 9671949]

Schectman. The mechanics of amphibian gastrulation. I. Gastrulation-producing interactions between various regions of an anuran egg (*Ityla regila*). Univ Calif Publ Zool 1942;51:1–39.

Schrijver I, Liu W, Odom R, Brenn T, Oefner P, Furthmayr H, Francke U. Premature termination mutations in FBN1: distinct effects on differential allelic expression and on protein and clinical phenotypes. Am J Hum Genet 2002;71:223–37. [PubMed: 12068374]

Shih J, Keller R. Cell motility driving mediolateral intercalation in explants of Xenopus laevis. Development 1992a;116:901–14. [PubMed: 1295743]

Shih J, Keller R. Patterns of cell motility in the organizer and dorsal mesoderm of Xenopus laevis. Development 1992b;116:915–30. [PubMed: 1295744]

Skoglund P, Dzamba B, Coffman CR, Harris WA, Keller R. Xenopus fibrillin is expressed in the organizer and is the earliest component of matrix at the developing notochord-somite boundary. Dev Dyn 2006;235:1974–83. [PubMed: 16607639]

Zhang H, Hu W, Ramirez F. Developmental expression of fibrillin genes suggests heterogeneity of extracellular microfibrils. J Cell Biol 1995;129:1165–76. [PubMed: 7744963]

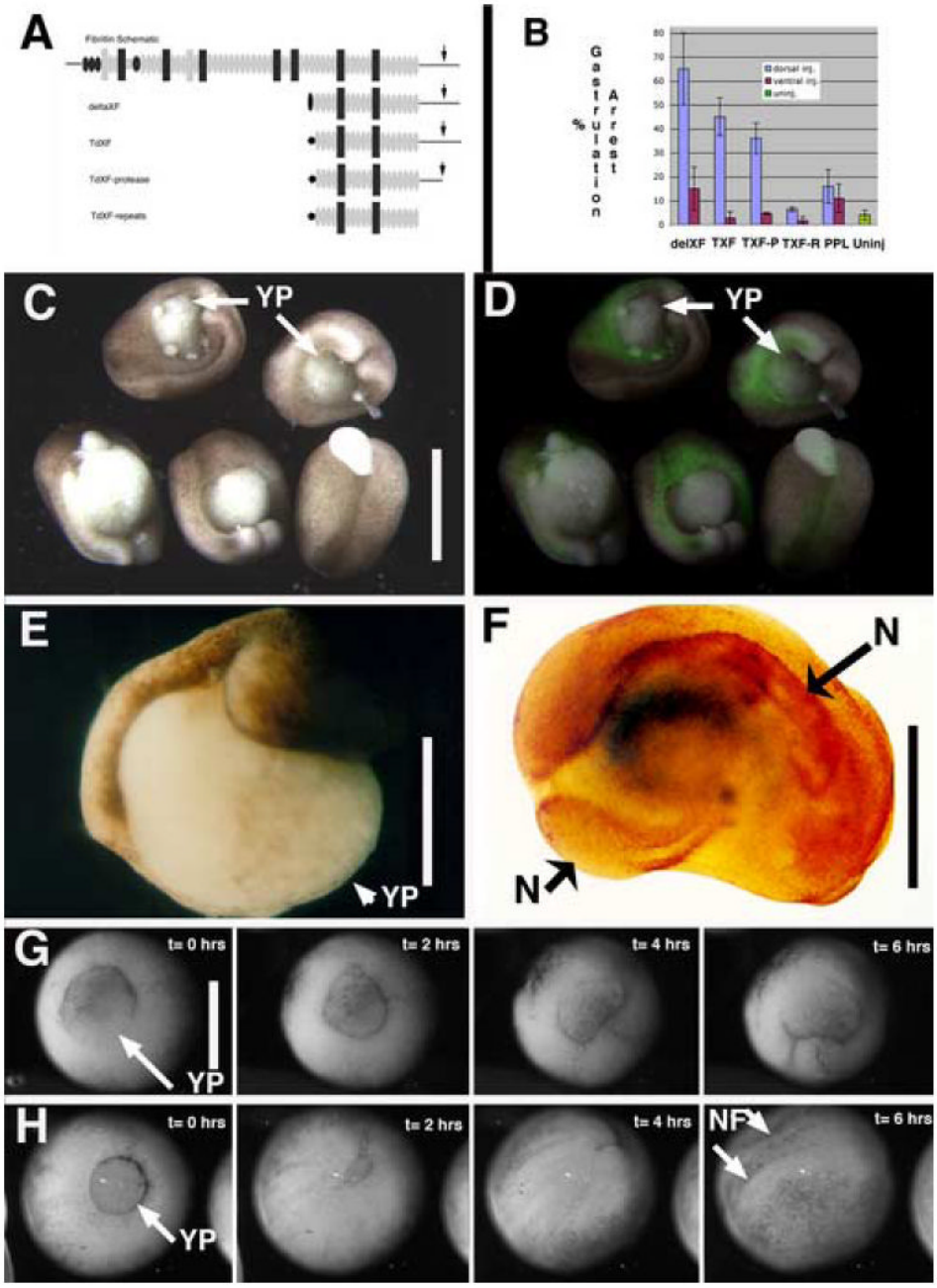

Figure 1. deltaXF/ TdXF expression perturbs gastrulation

A) Schematic outline of the domain structure of the prototypical fibrillin and the injection constructs: deletion XF (deltaXF), twice- deleted XF(TdXF) (similar to deltaXF but with a partial EGF repeat removed), and two carboxy-terminal deletions of TdXF, TdXF-Protease (TdXF-P), and TdXF-Repeats (TdXF-R). Shown are calcium binding EGF-like repeats (gray ovals), EGF-like repeats (black ovals), 8-cysteine repeats (black rectangles), hybrid repeats between EGF-like and 8-cysteine repeats (gray rectangles) unique sequences (lines and gray box), N-cad signal sequences (black oval and pentagon- representing two distinct fusion sites between signal sequence and XF sequence) and furin processing site (arrow). B) Percent of embryos exhibiting open blastopores is plotted with SEM for presumptive dorsal vs. ventral

mesoderm injection of deltaXF (D, n= 56; V, n=49), TdXF (D, n=77 ; V, n=80), TdXF-P (D, n=71 ; V, n=71), TdXF-R (D, n=75 ; V, n=59), pre-prolactin (PPL) (D, n= 47; V, n= 44), or uninjected embryos (n=195). C) DeltaXF dorsally injected late gastrula embryos exhibiting failure of blastopore closure and partial exogastrulation. Scale bars are 0.5 mm in C-H. D) The same embryos as in C, but visualizing co-injected GFP to reveal the dorsal targeting of these injections. E) Dorsal deltaXF injected St 22 embryo exhibiting open blastopore. F) deltaXF injected embryo stained for a notochord marker (Tor70), which reveals notochord (N) ringing the yolk plug. G and H) Frames from movies of developing embryos injected with G) TdXF or H) PPL with elapsed time indicated. YP = yolk plug; N = notochord; NF = neural folds.

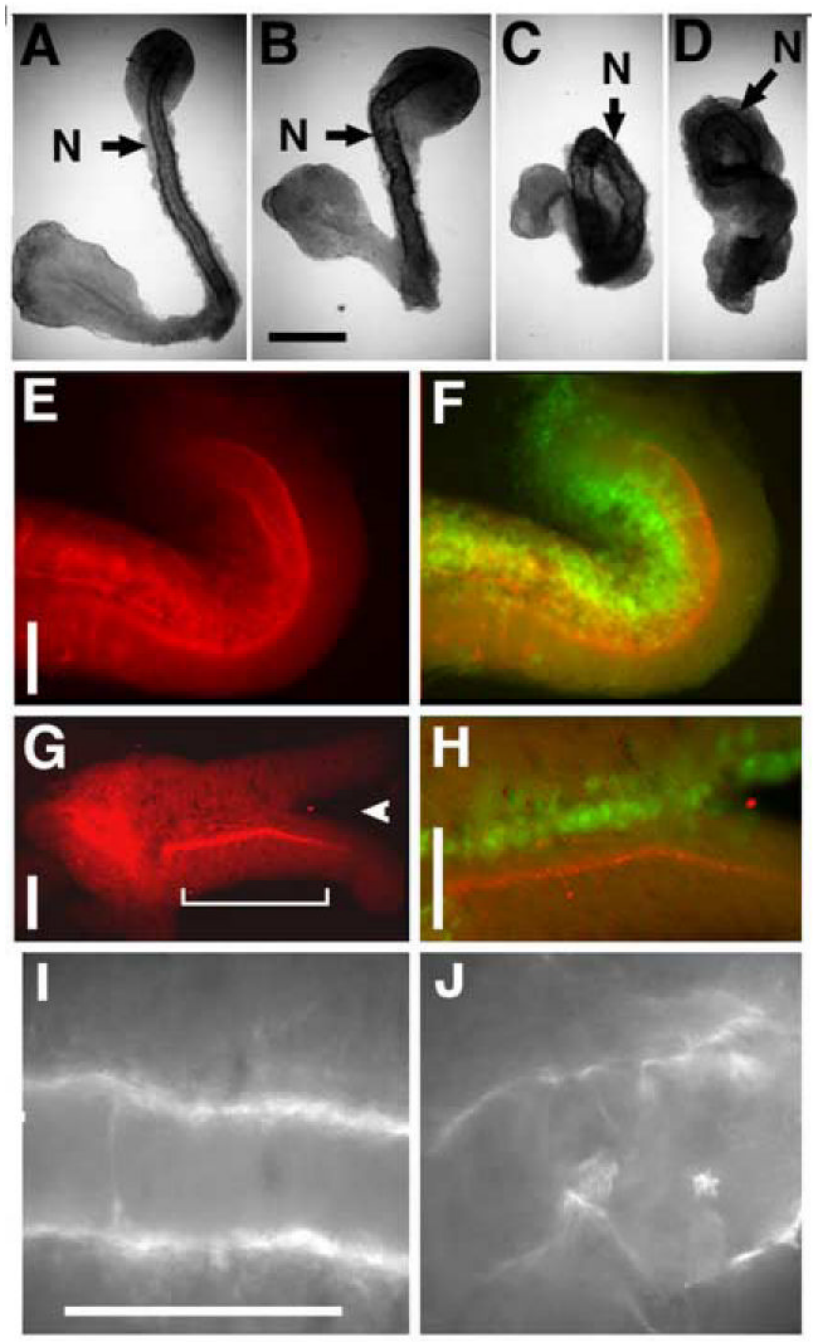

Figure 2. Morphology and XF fibrils in deltaXF expressing explants

A- D) Keller sandwiches made from embryos injected with increasing doses of deltaXF, allowed to extend and stained for notochord (N). Scale bar in B is 0.2 mm. A) Control sandwich from uninjected embryos (representative example shown, n=5), B-D) 0.5 ng, 1 ng, and 2 ngs deltaXF RNA per dorsal blastomere, respectively (n= 3, 3 and 5 respectively). E-H) explants stained for native XF immunoreactivity (E and G), and both native fibrils (red) and GFP (green), indicating the region of delXF expression, with yellow being the combined signal (F and H). Arrowhead in G indicates bifurcation of explant, and bracket indicates region shown in H. Scale bars are 0.1 mm in E-J. I) XF fibrils around notochord of an uninjected open face explant, and J) XF fibrils in notochord region of explant globally expressing deltaXF.

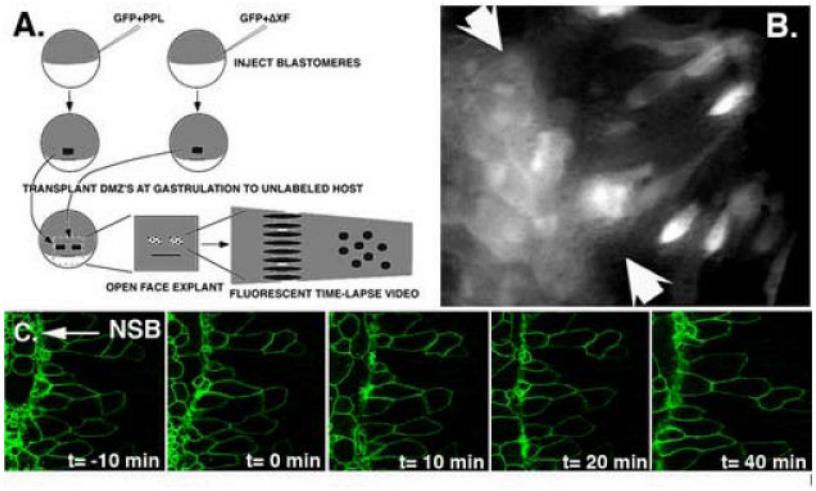

Figure 3. Effect of deltaXF expression and CB1 peptide on cell behavior

A and B) Genetic mosaic transplantation analysis of deltaXF expressing cells reveals that deltaXF expression perturbs notochordal cell behaviors. A) Embryos injected with either GFP and deltaXF or GFP and pre-prolactin were used to make DIMZ explants, and two small groups of expressing cells, one from each type of injected embryo, were transplanted above the dorsal lip of a single host embryo at mid-gastrulation. After healing, the DIMZ of this host embryo was explanted into culture and the labeled control and experimentally injected cells were observed during extension. B) A single frame from a movie showing morphology of GFP labelled, transplanted control cells (injected with pre-prolactin + GFP - right of arrows) or experimentally injected (deltaXF + GFP - left of arrows) cells in an extending explant. Cells that exhibit an elongate morphology fit the profile of a MIB expressing cell, and most control cells have length-to-width ratios greater than 2, in contrast to deltaXF expressing cells in the same explant. In addition, note that the experimentally injected graft has maintained its cohesion during extension of the host explant, in contrast to the control injected graft which has been broken up through the process of intercalation to generate intermixed labeled and unlabeled cells. This serves as a positive control for this experiment, indicating that the grafted cells can participate in morphogenesis. C) CB-1 peptide does not affect notochordal cell behavior. Time-lapse frames visualizing notochordal cell behavior in an axial explant undergoing morphogenesis to which CB-1 peptide is added at 50 ug /ml at frame t=0. In contrast to deltaXF expression above, notochordal cell behavior is not affected by acute application of the CB-1 peptide.

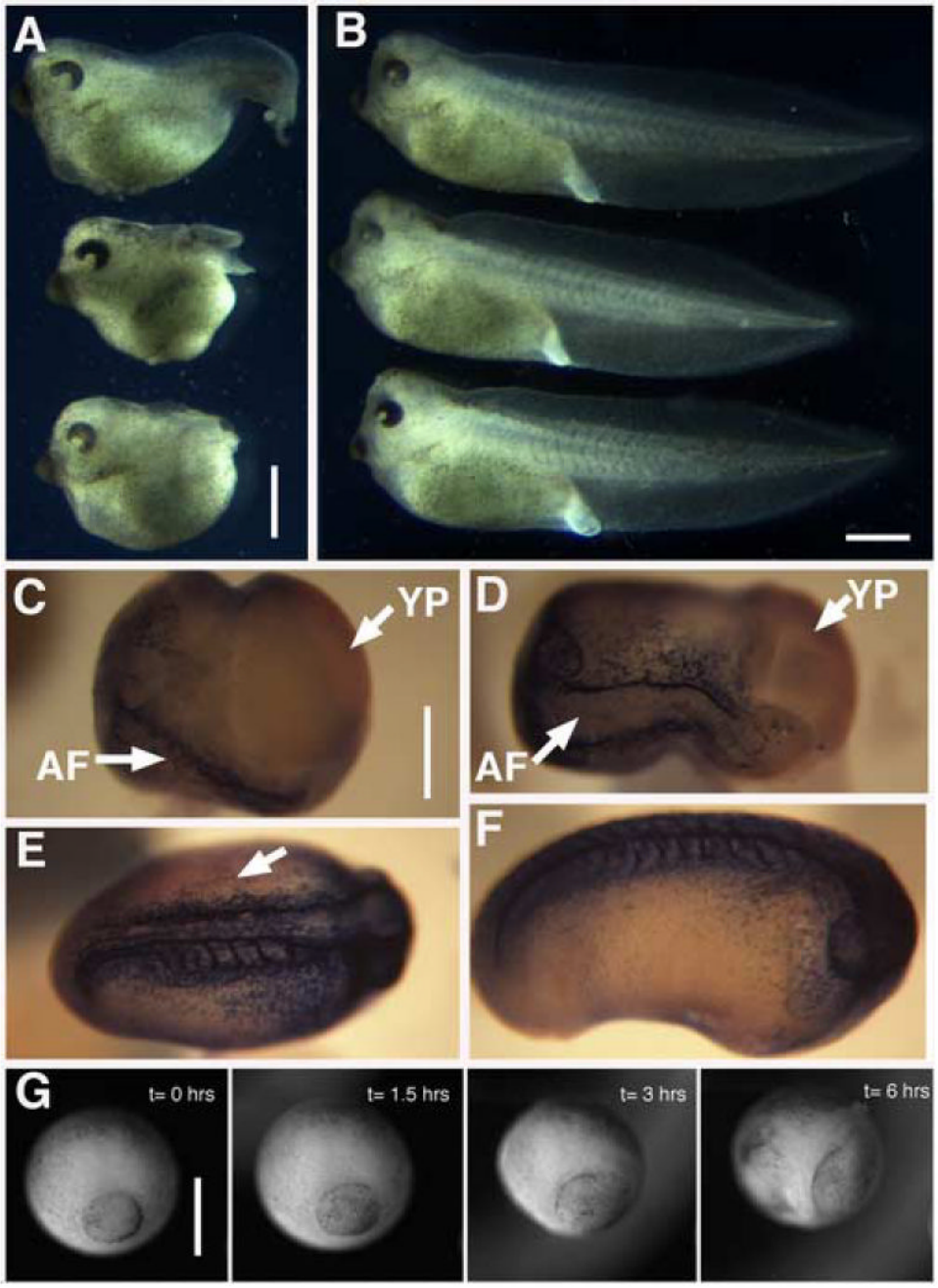

Figure 4. Effect of CB-1 peptide on development

A) CB-1 injected embryos exhibit marked axis shortening and open blastopores. B) Sibling embryos to those in A) injected with scrambled peptide develop normally. Scale bars in A and B are are 1 mm. C-F) Embryos injected with 300 ng CB-1 peptide exhibiting graded levels of gastrulation arrest that correlates with fibrillin antibody staining. Scale bar for C-F is 0.5 mm. C) An injected embryo exhibiting strong gastrulation arrest exhibits little fibrillin staining and a large open blastopore, and will develop into an embryo such as shown in A). D) An embryo that is progressively better at closing its blastopore exhibits progressively more fibrillin staining. The majority of injected embryos appear like those in C) or D). E) Embryos that do close their blastopore can exhibit fibrillin staining defects, such as the somitic staining on only

one side seen in dorsal view here (Side lacking fibrillin staining indicated by arrow). F) A few injected embryos exhibit normal fibrillin staining,, but still exhibit a slightly abnormal morphology. G) Time-lapse sequence showing failure of blastopore closure in an injected embryo; compare to Fig 1H for normal closure. Scale bar is 0.5 mm. AF = axial fibrillin staining; YP = yolk plug.

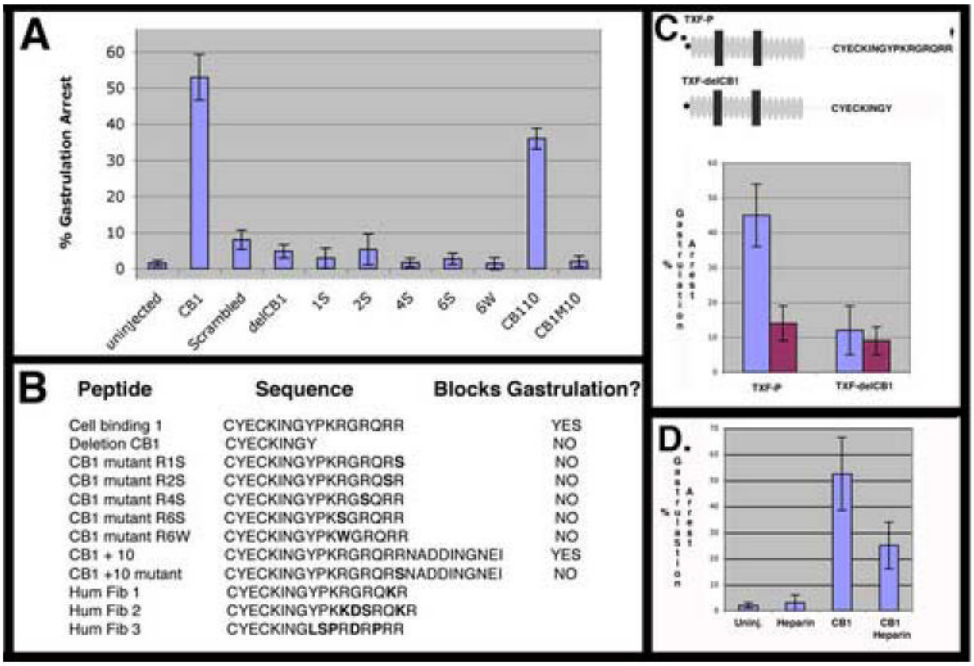

Figure 5. Functionally defining the CB-1 domain responsible of perturbing gastrulation

A) Percent of gastrulation arrested embryos is plotted with SEM from at least three experiments for uninjected embryos (n= 273), or injected with CB-1 peptide (n= 205), scrambled peptide (n=272), deletion CB1 peptide (n=84), CB1M1S (n= 68), CB1M2S (n= 76), CB1M4S (n= 58), CB1M6S (n= 74). CB1M6W (n= 72), CB1+10 (n= 139), CB1M10 (n= 50). B) Table of sequences of injected peptides. Mutations from CB-1 sequences are shown in bold. C) Injection of an mRNA encoding a deletion mutant of the TXF-P construct that lacks a functional CB-1 domain does not perturb gastrulation. Domain structure key is as in Fig. 1. Injection of TXF-P on the dorsal (n=40) but not ventral (n=43) side of the embryo causes gastrulation arrest. In contrast, expressing an eight amino acid deletion variant, TXF-delCB1, does not cause gastrulation arrest when injected dorsally (n= 42) or ventrally (n= 34). D) The gastrulation arrest phenotype of the CB1 peptide is heparin sensitive. Failure of blastopore closure is plotted for uninjected embryos (n=75), embryos injected with 30 nl of 200 ug/ml heparin (n=66), injected with 30 nl of 10 mg/ml CB-1 (300ng) peptide (n=80), or injected with CB-1 peptide (300 ng) preincubated with 200 ug/ml heparin (n=81).

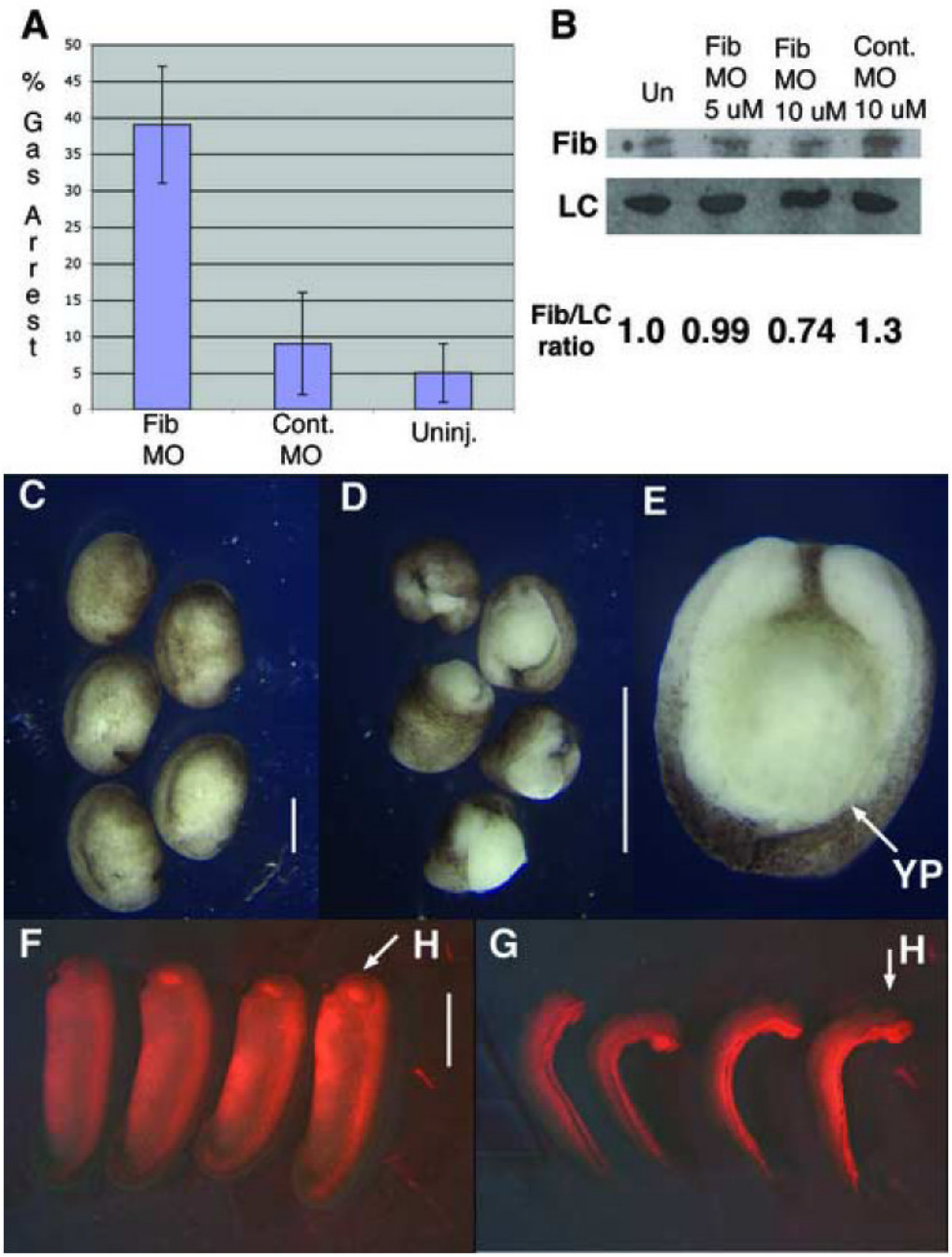

Figure 6. XF morpholino perturbs gastrulation

Reducing XF translation in embryos blocks the normal progression of gastrulation. A) Percent of gastrulation arrested embryos is plotted with SEM for XF morpholino (n=93), control MO (n=88), or uninjected embryos (n=94). B) Western blot for XF reveals XF morpholino injection results in a partial knockdown of XF protein levels, when mormalized against a loading control (LC). C) Embryos injected with 10 uM 5-misprime XF control morpholino develop normally. D and E) Embryos injected with 10 uM XF MO exhibit open blastopores. F) Embryos unilaterally injected with 10 uM 5-misprime control morpholino do not bend. G) Embryos injected with 10 uM XF morpholino bend towards the injected side. H = head; YP = yolk plug.

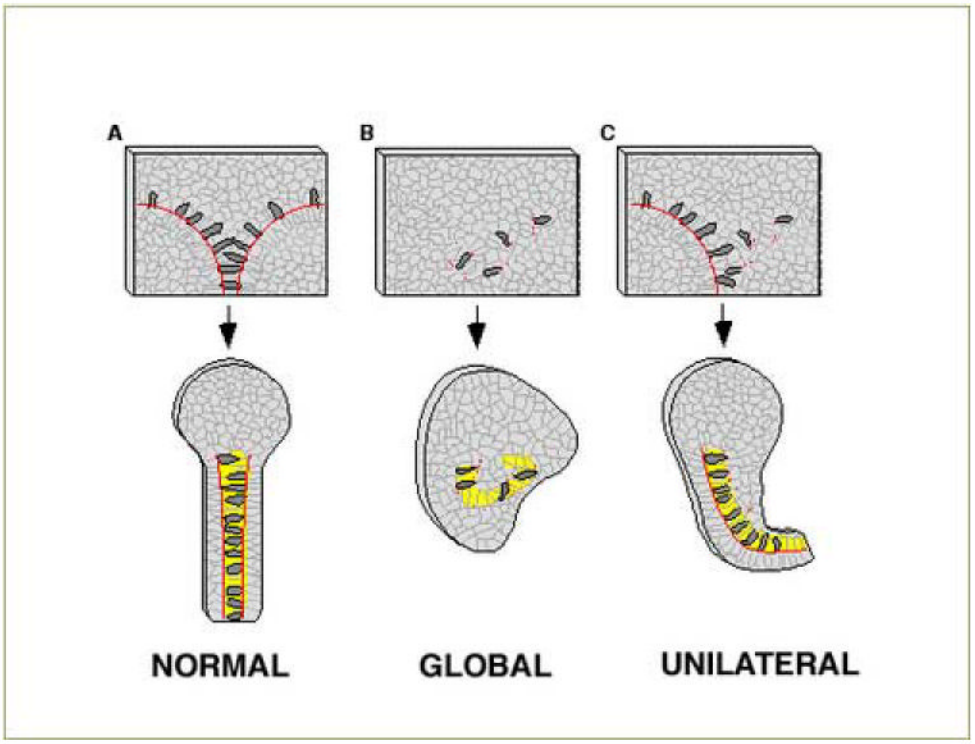

Figure 7. Model for function of Xenopus fibrillin in convergence and extension, and consequences for mophogenesis of perturbing XF globally and unilaterally

All panels show an open face DIMZ explant before and after autonomous extension. For each, extension is downward (posterior) with yellow representing notochord and red lines indicating the location of the presumptive notochordal-somitic boundary (upper panels),or the localization of XF in the mature, matrix-rich notochordal-somitic boundary (lower panels). A) In normal open face DIMZ explants cells (open circles) are induced to 36 become bilaterally protrusive and elongate (exhibit MIB), bind to the XF containing notochord-somite boundary, where they exhibit local inhibition of protrusion. These cells then converge towards the midline, dragging the boundary with them and causing directed extension of the notochord (shown in the extended explant). In this model XF at the boundary functions in the process of directing extension posteriorly, and may function in regulating cell motility at the boundary. B) In explants in which XF deposition at the boundary is globally perturbed, either by expressing deltaXF widely or injecting the CB-1 peptide, fibrillin fibril localization to both of the bilateral boundaries is disrupted. This leads to twisted notochords as extension is no longer globally directed in the posterior direction, and in whole embryo experiments leads to failure of blastopore closure. C) In explants in which XF is compromised unilaterally bending occurs, again suggesting that XF fibrils normally function to direct extension posteriorly.